RGD-MODIFIED SUNITINIB LIPOSOME TO IMPROVE THE THERAPEUTIC EFFICIENCY OF RENAL CARCINOMA

Huibing Li[1,2*] Shimiao Zhu[1], Qi Li[1], Zongsu Zhang, Changyi Quan[1,*]
[1]Department of Urology, Tianjin Institute of Urology, The Secondary Hospital of Tianjin Medical University. No.23 Pingjiang road, Hexi district, Tianjin, 300211, China - [2]Department of Urology, The First Affiliated Hospital, and College of Clinical Medicine of Henan University of Science and Technology, Luoyang 471003, China

ABSTRACT

Objective: *Renal carcinoma is a very high degree of malignancy with a very high incidence and mortality. Angiogenesis of renal carcinoma is very important for tumor metastasis and prognosis. Inhibition of this process can be more effective against renal carcinoma. To overcome the limitations of sunitinib for treating renal carcinoma, in this study, we developed a RGD-modified liposomal drug delivery system.*

Methods: *The liposomes were prepared and characterized for particle size, zeta potential, encapsulation efficiency, release profile, stability, and hemolysis. The enhanced target and anti-angiogenesis effects were also studied in vitro and in vivo.*

Results: *The results suggested that the RGD-modified liposome (S/RGDL) obviously suppressed the proliferation capacity both in vitro and in vivo compared to naked sunitinib and non-coated liposome (S/L), which might be due to the dual-antiangiogenesis of both sunitinib and RGD peptide.*

Conclusion: *This work presented a way that S/RGDL may be used as potential means to improve the therapeutic efficiency of renal carcinoma via enhancing target and anti-angiogenesis ability.*

Keywords: *Renal carcinoma, angiogenesis, RGD peptide, sunitinib, liposome.*

DOI: 10.19193/0393-6384_2023_5_158

Received *January 15, 2023;* ***Accepted*** *May 20, 2023*

Introduction

Renal carcinoma is a very high degree of malignancy, with a very high incidence and mortality[1, 2]. The diagnosis and treatment are very difficult for malignant tumors of the digestive tract. In recent years, the 5-year overall survival rate of renal carcinoma is decreasing radically, which is the malignant tumor with the worst prognosis[3]. It is difficult to be diagnosed effectively in the early stage, while the advanced stage has a high degree of metastasis and heterogeneity. Therefore, in order to improve the prognosis of renal carcinoma patients, it is urgent to develop new and more effective ones. Angiogenesis refers to the process of forming new blood vessels through budding from existing capillaries, mainly including basement membrane degradation, activation, proliferation and migration of endothelial cells, reformation of tubular structure, basement membrane reconstruction and vascular network formation, which is a complex physiological process involving a variety of molecules[4-6]. Angiogenesis needs to be regulated by both angiogenic and inhibitory factors[7]. Tumor angiogenesis is very complex, but in renal carcinoma, which is a highly malignant tumor, angiogenesis is dense and grows rapidly[8, 9]. Angiogenesis of renal carcinoma is very important for tumor metastasis and prognosis[10]. Inhibition of this process can be more effective against renal carcinoma. Sunitinib, developed by Pfizer, is a multi-target angiogenesis inhibitor that inhibits the activity of various tyrosine

kinases, including VEGFR1, FGFR1, PDGFR, and c-kit[11]. It is widely used to treat the renal carcinoma, pancreatic cancer, and other cancers[12-14]. But, as the inherent limitation of chemotherapeutic drugs, sunitinib has limited targeting ability and distribution in the whole body. Although increasing the dose of drugs in treatments may increase the concentration of the tumors, it could cause stronger side effects and severer toxicity. Hence, a huge amount of demand, not only for sunitinib but in general, strategies are urgently needed.

It is well known that RGD peptide is one of the most frequently-used neoplastic targeting ligands in drug delivery systems[15]. The RGD sequence, an arginine-glycine-aspartic (Arg-Gly-Asp) tripeptide, has been shown to be the most promising ligand for targeting most of the malignant tumors, including renal carcinoma, breast cancer, bone metastasis and other human cancers. As a result, many researchers have done a lot of interesting work on the nanocarriers that are modified with RGD peptide to deliver the drugs to the tumors[15, 16]. In addition, the integrin receptor αvβ3 is also over-expressed on the neovascularization endothelial cells[17, 18], so that the RGD peptide may have the property of targeting the tumor neovascularization.

What's more, the tumor endothelial cells also have an over-expression of integrin αvβ3, which is associated with cell growth, migration, tumor invasion, proliferation, metastasis, and angiogenesis[19], so the αvβ3 can be an attractive target for antitumor therapy. Many integrin antagonists, including RGD peptides, antibodies, and recombinant proteins, induce tumor degeneration by decreasing angiogenesis and increasing apoptosis of tumor endothelial cells. For example, the RGD peptide Cilengitide has been used to treat the renal carcinoma, glioma, and prostate cancer via blocking angiogenesis, tumor formation, and tumor metastasis[20, 21]. To overcome the limitations of chemotherapy for treating renal carcinoma, in this study, we developed a RGD-modified liposomal drug delivery system. The liposome was capable of recognizing the receptor of integrin αvβ3 over-expressed on the cancer cell and neovascularization endothelial cells via RGD peptide on the surface of the particles, which could enhance the cellular uptake of renal carcinoma cells.

What's more, the RGD-modified and non-coated liposomes were prepared by the lipid film hydration ultrasound method, and the characteristics, targeting abilities, and pharmacodynamics of dual-antiangiogenesis of both sunitinib and RGD peptide were evaluated in vitro and in vivo.

Materials and methods

Chemistry

Synthesis of intermediates 2

To a solution of compound 1 (2.30 g, 13.13 mmol) in CH_2Cl_2 (50 mL) were added N-methylmorpholine (NMM, 1.47 mL, 13.13 mmol) and isobutyl chlorocarbonate (IBCF, 1.66 mL, 13.13 mmol), and the reaction was stirred at -15 oC for 10 min. Then, Asp(OBn)-OBn (4.11 g, 13.13 mmol) in CH_2Cl_2 (20 mL) was added slowly.

The mixture was stirred for another 10 h at r.t. and washed with 1 mol/L HCl (50 mL), saturated $NaHCO_3$ (50 mL), and saturated NaCl (50 mL). The organic layer was dried with anhydrous Na_2SO_4 and concentrated in vacuo. The residue was purified by flash column chromatography to get compound 2 (4.51 g, 73%) as white waxy solid. Mp: 87-89 °C. HRMS: (ESI+) calculated for $C_{25}H_{30}N_2O_7Na$ $[M+Na]^+$ 493.1951, found 493.1955. Elemental Analysis: C, 63.82; H, 6.43; N, 5.95, found C, 63.70; H, 6.61; N, 5.84.

Synthesis of intermediates 3

Compound 2 (2.00 g, 4.25 mmol) was dissolved in HCl/THF (25%, 5 mL), and the mixture was stirred at room temperature for 1 h. After removing the solvent, the residue was redissolved into 30 mL ethyl acetate. Then, the mixture was washed with saturated $NaHCO_3$ (50 mL × 2) and saturated NaCl (50 mL × 2). The organic layer was dried with anhydrous Na_2SO_4 and concentrated in vacuo.

The residue was purified by flash column chromatography to give compound 3 (1.42 g, 90%) as colorless oil. HRMS: (ESI+) calculated for $C_{20}H_{22}N_2O_5Na$ $[M+Na]^+$ 393.1426, found 393.1422. Elemental Analysis: C, 64.85; H, 5.99; N, 7.56, found C, 64.74; H, 6.13; N, 7.39.

Synthesis of intermediates 4

To a solution of Boc-Arg(NO_2)-OH (1.50 g, 4.70 mmol) in 20 mL DMF were added NMM (0.52 mL, 4.70 mmol) and IBCF (0.60 mL, 4.70 mmol), and the mixture was stirred at -15 °C for 10 min. Then, compound 3 (1.74 g, 4.70 mmol) in DMF (5 mL) was added slowly. The reaction was continued to stir for another 5 h at r.t. Subsequently, the DMF was removed, and 60 mL ethyl acetate was added to

dissolve the residue. The mixture was washed with 1 mol/L HCl (50 mL × 2), saturated $NaHCO_3$ (50 mL × 2), and saturated NaCl (50 mL × 2), and the organic layer was dried with anhydrous Na_2SO_4 and concentrated in vacuo.

The residue was purified by flash column chromatography to get compound 4 (2.05 g, 65%). HRMS: (ESI+) calculated for $C_{32}H_{41}N_7O_{10}Na$ $[M+Na]^+$ 694.2813, found 694.2815. Elemental Analysis: C, 55.43; H, 6.15; N, 14.60, found C, 55.36; H, 6.24; N, 14.48.

Synthesis of intermediates 5

To a solution of compound 4 (1.00 g, 1.49 mmol) in CH_2Cl_2 (20 mL) was added trifluoroacetic acid (TFA, 5 mL), and the reaction was stirred for 2 h at room temperature.

Then, the mixture was washed with saturated $NaHCO_3$ (50 mL × 2) and saturated NaCl (50 mL × 2). The solvent was removed to obtain the compound 5 (0.72 g, 85%), which was used for the next step without further purification. HRMS: (ESI+) calculated for $C_{26}H_{33}N_7O_8Na$ $[M+Na]^+$ 594.2288, found 594.2285. Elemental Analysis: C, 54.63; H, 5.82; N, 17.15, found C, 54.78; H, 5.70; N, 17.22.

Synthesis of intermediates 6

To a solution of succinic anhydride (0.50 g, 5.00 mmol) in dioxane (5 mL) was added compound 5 (1.90 g, 3.33 mmol) slowly, and the reaction was stirred at 80 °C for 0.5 h. Then, the mixture was concentrated in vacuo, and the residue was purified by chromatography to yield 6 (1.54 g, 69%) as a white solid. HRMS: (ESI+) calculated for $C_{30}H_{37}N_7O_{11}Na$ $[M+Na]^+$ 694.2449, found 694.2446. Elemental Analysis: C, 53.65; H, 5.55; N, 14.60, found C, 53.78; H, 5.66; N, 14.69.

Synthesis of intermediates 8

To a solution of compound 7 (5.00 g, 12.93 mmol) in 20 mL pyridine was added the solution of TsCl (3.70 g, 19.40 mmol) in pyridine (10 mL), then the mixture was stirred at 50 °C for 10 h. The solvent was removed, and the residue was redissolved with 100 mL ethyl acetate. The mixture was washed with 1 mol/L HCl (50 mL × 2) and saturated NaCl (50 mL × 2). The solvent was removed to get compound 8 (6.29 g, 90%), which was used for the next step without further purification. Mp: 128-130 °C. HRMS: (ESI+) calculated for $C_{34}H_{52}O_3S$ Na $[M+Na]^+$ 563.3535, found 563.3537. Elemental Analysis: C, 75.51; H, 9.69; S, 5.93, found C, 75.59; H, 9.55; S, 5.82.

Synthesis of intermediates 9

To a solution of compound 8 (2.00 g, 3.70 mmol) in dioxane (20 mL) was added pentaethylene glycol (6.26 mL, 29.58 mmol), then the reaction was allowed to reflux for 10 h.

The solvent was removed, and the residue was redissolved with 50 mL dichloromethane. The mixture was washed with saturated NaCl (50 mL × 2). After removing the CH_2Cl_2, the residue was purified by chromatography to give compound 9 (1.17 g, 52%) as a colorless oil. HRMS: (ESI+) calculated for $C_{37}H_{66}O_6Na$ $[M+Na]^+$ 629.4757, found 629.4752. Elemental Analysis: C, 73.22; H, 10.96, found C, 73.35; H, 10.84.

Synthesis of intermediates 10

To a solution of compound 6 (0.85 g, 1.27 mmol) in 20 mL CH_2Cl_2 were added dicyclohexylcarbodiimide (DCC, 0.31 g, 1.52 mmol) and dimethylaminopyridine (DMAP, 16 mg, 0.13 mmol), and the mixture was stirred at -5 °C for 10 min. Then, the compound 9 (0.77 g, 1.27 mmol) in CH_2Cl_2 (5 mL) was added slowly.

The mixture was stirred for another 5 h at r.t. The reaction was terminated and then filtered. The filtrate was concentrated, and the residue was purified by flash chromatography to give 10 (1.25 g, 78%). HRMS: (ESI+) calculated for $C_{67}H_{101}N_7O_{16}Na$ $[M+Na]^+$ 1282.7202, found 1282.7207. Elemental Analysis: C, 63.84; H, 8.08; N, 7.78, found C, 63.69; H, 8.21; N, 7.84.

Synthesis of intermediates 11

To a solution of compound 10 (0.50 g, 0.40 mmol) in CH_3OH (10 mL) was added Pd/C (50 mg, 10%). Then, the mixture was stirred in a hydrogen atmosphere at 40 °C for 30 h. Pd/C was filtered, and the filtrate was concentrated to obtain ligand 11 (0.31 g, 75%). HRMS: (ESI+) calculated for $C_{53}H_{92}N_6O_{14}Na$ $[M+Na]^+$ 1059.6569, found 1059.6564. Elemental Analysis: C, 61.37; H, 8.94; N, 8.10, found C, 61.50; H, 8.82; N, 8.19.

Preparation of liposomes

The liposomes loading sunitinib were prepared according to the thin film hydration method[22, 23].

The component ratio was optimized as follows:

• Conventional liposome (L), SPC/cholesterol/ (molar ratio = 62: 33);

• RGD-modified liposome (RGDL), SPC/ cholesterol/ligand 11 (molar ratio = 62: 33: 3).

Briefly, the mixed solution of CH_2Cl_2/CH_3OH (v/v = 2:1) was used to dissolve all the lipid materials, and then the solvent was removed on a rotary evaporator at 37 °C to form a thin film, which was further dried in vacuum for 10 h. After hydrating with PBS (pH 7.4) at 20 °C for 30 min, the solution was sonicated intermittently at 80 W for 80 s to obtain the liposomes. To the solution of lipids, was added the appropriate amount of sunitinib before removing the solvent to prepare sunitinib-loaded liposomes (S/L, S/RGDL).

The entrapment efficiency (EE%) and drug loading efficiency (DL%) of sunitinib were detected by high-performance liquid chromatography (HPLC). The detection was performed on an Agilent 1200 HPLC with an ODS-C18 column (4.6 mm × 250 mm, 5 μm). The mobile phase included water-methanol (80/20, v/v) with a flow rate of 1.0 mL/min. 20 μL of the sample containing sunitinib was injected, and the detection wavelength was 384 nm. The EE% and DL% were calculated according to the equations: EE% = weight of encapsulated sunitinib /the total weight of sunitinib, DL% = weight of encapsulated sunitinib/the total weight of liposome. What's more, the size and ζ potential of S/L and S/RGDL were detected using Malvern Zeta sizer Nano ZS90.

Release study of S/L and S/RGDL in vitro

The release behavior of sunitinib from liposomes S/L and S/RGDL was analyzed through dialysis. In briefly, the sunitinib-loaded liposomes (S/L and S/RGDL) were put into a dialysis bag (MWCO = 8 000 - 14 000 Da) respectively, which was then placed in 50 mL PBS containing 0.1% Tween 80 (v/v) as release medium.

Afterward, the bags were placed into a shaker at 37 °C with a gentle oscillation (50 rpm). At 0 h, 1 h, 2 h, 4 h, 8 h, 12 h, 24 h, and 48 h, 0.1 mL sample was taken out and replaced with fresh medium. The release behavior of sunitinib from free sunitinib was also studied as a control. Then, the amount of sunitinib was tested through the HPLC method, as mentioned above.

Stability of S/L and S/RGDL in vitro

The stability of liposomes S/L and S/RGDL was studied by investigating the turbidity variations in the presence of fetal bovine serum (FBS).

Both of the liposome formulations were mixed with an equal volume of FBS respectively, and then co-cultured at 37 °C with continuous shaking (50 rpm). The transmittance was measured between 0 h - 48 h on a microplate reader at 750 nm. The transmittance in PBS was defined as 100%.

Hemolysis assays

The fresh mouse blood was collected and centrifuged (5000 rpm) for 5 min to discard the supernatant. The precipitated mouse red blood cells were washed with PBS until the supernatant was colorless, and then the cells were re-suspended in PBS to the concentration of 2% (w/v).

Afterwards, the S/L and S/RGDL were diluted with PBS to get the liposome samples with different lipid concentrations at 10 nM, 25 nM, 50 nM, 100 nM, 200 nM, 400 nM. Subsequently, the sample (0.4 mL) was mixed with the red blood cells solution (0.1 mL), and then the mixture was co-incubated at 37 °C for 2 h with gentle shaking (50 rpm). After centrifuging at 10 000 rpm for 10 min, the absorbance of the supernatant was measured on a microplate reader at 540 nm. The hemolysis rate of each sample was calculated as percent hemolysis (%) = $(A_{Sample}-A_{Negative})/(A_{Postive}-A_{Negative}) \times 100\%$. The absorbance of PBS and Triton X-100 mixed with cells solution was defined as 0% and 100%, respectively.

MTT assays

UM-UC-14 cells were maintained in our lab, while human umbilical vein endothelial cells (HUVECs) were obtained from ATCC, and maintained in DMEM and RPMI-1640 medium, respectively, supplemented with 10% fetal bovine serum (FBS) at 37 °C in a 5% CO_2 incubator.

The MTT assays were performed according to the previous reported methods[24-26].

UM-UC-14 cells were seeded into the 96-well plates with a density of approximately 1000 cells each well and maintain for approximately 48 hours. Sunitinib-loaded liposomes (S/L and S/RGDL) and free sunitinib were diluted to predetermined concentrations with PBS and added into each well. The final concentrations of sunitinib were in the range of 10-200 μg/mL. After 24 h incubation, the cells were subsequently treated with MTT agent for 4 hours and washed with PBS for three times. Cells were then isolated by the use of 200 μL DMSO, and the OD value at the wavelength of 490 nm was measured and analyzed.

Tube formation assay

HUVECs were treated with control or sunitinib-loaded liposomes (S/L and S/RGDL) and free sunitinib (25 μM) and plated into a 24-well

plate precoated with Matrigel (1:1 dilution with RPMI-1640 medium). Images were obtained at the indicated times with a fluorescence microscope (Carl Zeiss, Jena, Germany), and the degree of tube formation was quantified by measuring the total tube length and number of nodes.

Wound healing assays

UM-UC-14 cells were treated with control or sunitinib-loaded liposomes (S/L and S/RGDL) and free sunitinib (25 μM) and grown for 24 hours. The cells were then wounded by scraping with a 200-μL pipette tip, followed by washing.

Subsequently, a complete culture medium was added to induce wound healing. Images were taken at 0 h and 24 h to evaluate the extent of cancer cell migration.

In-vivo acute toxicity

The acute toxicity of the three sunitinib formulations was investigated using BALB/c mice weighing 20-24 g. The mice were randomly divided into groups (n = 10). Before the study, the animals were abstained from food for 12 h, but they had free access to water. The different sunitinib formulations were injected into animals at the dose of 50, 100, 500, and 1000 mg/ Kg body weight via the tail vein. After 24 h, the dead animals were counted in each group. The animals were under observation for another two weeks for any morbidities or mortalities.

Tumor growth assays

All animal experiments in this study were approved by our laboratory animal ethics committee. Four weeks old BALB/c nude mice were bought from the Animal core facility. For tumor growth assay, UM-UC-14 cells were mixed with matrigel (BD Company) with a ratio of 2:1 and subcutaneously implanted into nude mice to induce tumors.

To detect the in vivo anti-tumor effects of the indicated drugs on UM-UC-14 xenografts, the mice were divided into 3 groups (n = 6 for each group); sunitinib, S/L, or S/RGDL was administrated via vein injection every 3 days at a dose of 10 mg/ kg sunitinib. After another 12 days, the tumors were isolated from the mice, and the weight was measured. What's more, the Immunoblot assays were performed to detect the expression of proteins.

Immunoblot assay

Tumor tissue samples were isolated from mice to extract the indicated proteins and separated by SDS-PAGE, sequentially transferred onto the NC membranes, followed by blocking with 5% fat-free milk in TBST buffer. NC membranes were subsequently treated with primary antibodies targeting a series of proteins, including CD31, VEGF, and β-actin, at room temperature for 1.5 hours. Subsequently, the membranes were incubated with secondary antibodies, which were HRP-conjugated at room temperature for 50 minutes. Signals were then visualized by the use of an ECL kit.

Statistical analysis

All the data were presented as mean ± standard deviation (SD). The statistical analyses were conducted using GraphPad Prism 6.0 (San Diego, CA, USA). Statistical comparisons were performed by analysis of variance (ANOVA) for multiple groups followed by Student's t-test. The significance was defined as follows: $^{*}P<0.05$, $^{**}P<0.01$, $^{***}P<0.001$.

Results

Chemistry

The synthetic pathway of liposome ligand 11 was outlined in Figure 1. Briefly, the cancer-targeting tripeptide RGD with carboxyl groups protected by benzyl groups was synthesized by a conventional liquid-phase peptide synthetic method.

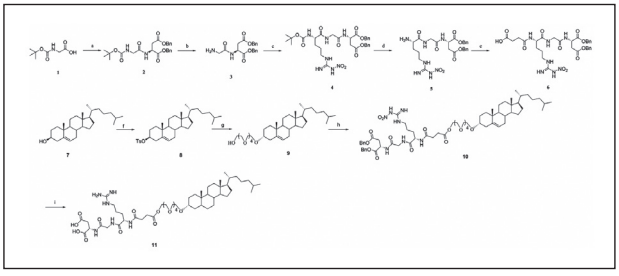

Figure 1: Synthesis of liposome ligand 11. Reagents and conditions: (a) Asp(OBn)-OBn, IBCF, NMM, CH2Cl2, -15 oC - r.t., 5 h. (b) HCl, THF, r.t., 1 h. (c) Boc-Arg(NO2)-OH, IBCF, NMM, DMF, -15 oC - r.t., 5 h. (d) TFA, CH2Cl2, r.t., 2 h. (e) succinic anhydride, dioxane, 80 oC, 0.5 h. (f) TsCl, pyridine, 50 °C, 10 h. (g) Pentaethylene glycol, dioxane, reflux, 10 h. (h) 6, DCC, DMAP, CH2Cl2, -5 oC - r.t., 10 h. (i) H2, Pd/C, CH3OH, 40 oC, 30 h.

Condensation of the available material Boc-Gly and Asp(OBn)-OBn in the presence of IBCF and NMM gave the dipeptide intermediate 2, which was then removed from the Boc group to generate the ammonia 3. Subsequently, the compound 3 was coupled with Boc-Arg(NO_2)-OH to obtain RGD tripeptide 4, and then removing the Boc protecting

group and coupling with succinic anhydride to get the acidic RGD 6. What's more, cholesterol 7 was esterified with TsCl, followed by etherification with pentamethylene glycol to generate the alcohol 9. Coupling the tripeptide RGD 6 with alcohol 9 in the presence of DCC and DMAP generated intermediate 10, which was deprotected with 10% Pd/C to obtain the desired ligand 11.

Characterization of liposomes

The proper sizes and uniform distribution were critical for the sunitinib-loaded liposomes to target the cancer and inhibit tumor angiogenesis.

The mean diameters and low polydispersity index (PDI) were detected through dynamic light scattering, and the result indicated that these liposomes had suitable size (about 110 nm) and PDI (about 0.2). Table 1 also showed that the EE% of the both liposomes was over 90% and DL% was about 3%. What's more, the weak negative ζ potential (about 0.2) of S/RGDL could decrease the absorption of the reticuloendothelial system and immune response.

	Size (nm)	PDI	EE (%)	DL (%)	Zeta potential (mV)
S/L	108.82±6.7	0.201±0.034	91.62±5.19	2.95±0.29	-3.57±0.44
S/RGDL	111.34±5.8	0.199±0.081	92.34±6.88	2.9 0.51	-6.81±0.83

Table 1: The characterization of S/L and S/RGDL (n = 3).

The release behavior study of liposomes was usually used to evaluate the entrapment, membrane flexibility and integrity, and affinity of carrier systems. It was exposed that the sunitinib from free sunitinib showed a fast release characteristic, with over 80% sunitinib being released in 12 hours (Figure 2A). While the sunitinib-loaded liposomes released about 50% loaded sunitinib within 12 hours, and the release exhibited a slow release rate afterward. Figure 2A also showed that neither of the two liposomes exhibited burst initial release patterns.

The stability of liposomes S/L and S/RGDL in physiological conditions is critical for the application in vivo. The transmittances of the two liposome formulations were over 90%, and they did not have obvious variation during the 48-h culture in FBS (Figure 2B). The results suggested that S/L and S/RGDL were stable enough, which was important for further study in vivo. The hemocompatibility of S/L and S/RGDL was estimated through hemolysis assays. It was shown that both of the liposomes had no significant increase in the hemoglobin release when the phospholipids were up to 400 nM (Figure 2C), which implied that they had a good biosecurity[27].

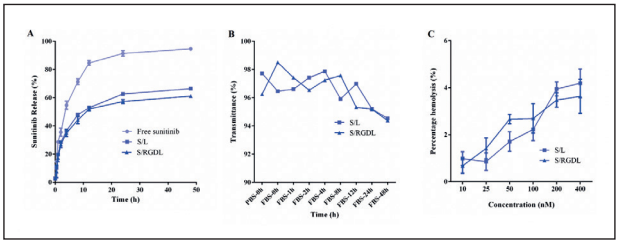

Figure 2: (A) TEM images of S/RGDL. (B) The sunitinib release profiles of free sunitinib, S/L, and S/RGDL in PBS (pH 7.4) containing 0.1% Tween 80 over 48 h. Both of the liposomes showed a slow release rate compared to the free sunitinib group. (C) The variations of transmittance of S/L and S/RGDL in 50% FBS. Neither of the liposomes have obvious variation during the 48-h culture in FBS. (D) Hemolysis percentage of liposomes S/L and S/RGDL in vitro. Both of the liposomes had obvious hemoglobin release when the phospholipids were up to 400 nM. (n = 3, mean ± SD).

Effect of sunitinib formulations on the proliferation, migration, and angiogenesis of renal carcinoma in vitro

We then assessed the effects of on the proliferative ability of UM-UC-14 cells through MTT assays. The results showed that sunitinib or S/L led to an increased cell death (%) from 10-200 μg/mL (concentration of sunitinib), and the treatment of S/RGDL more significantly increased the cell death (%), suggesting the critical effects of on cell proliferation (Figure 3).

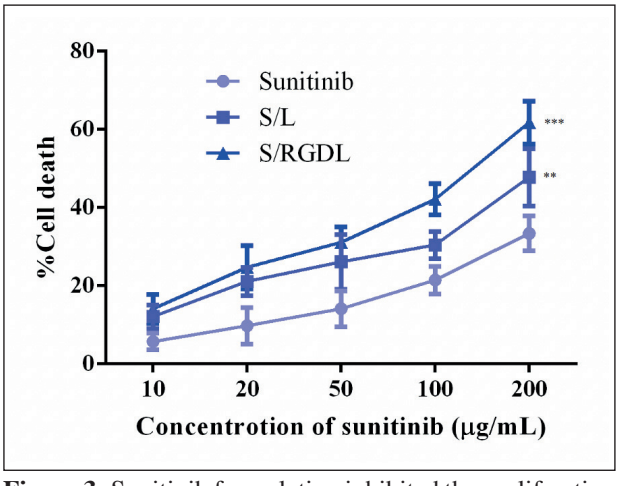

Figure 3: Sunitinib formulation inhibited the proliferation of UM-UC-14 cells in vitro. MTT assays were performed to detect the proliferation level in cells treated with sunitinib, S/L, or S/RGDL. Results are presented as mean

As tumor cell proliferation and migration are two key processes involved in tumorigenesis, we further investigated whether these sunitinib

formulations would affect UM-UC-14 cell migration through wound closure assays. As was expected, we found S/RGDL had a more obvious effect, compared to sunitinib or S/L, on the migration of UM-UC-14 cells (Figure 4A, B). Angiogenesis was a necessary process for tumor growth and development.

To investigate the possible effects of sunitinib or sunitinib liposomes on angiogenesis, we performed tube formation assays. Interestingly, we found that S/RGDL markedly impaired tube formation, compared to other groups (Figure 4C-E), suggestive of impaired angiogenesis.

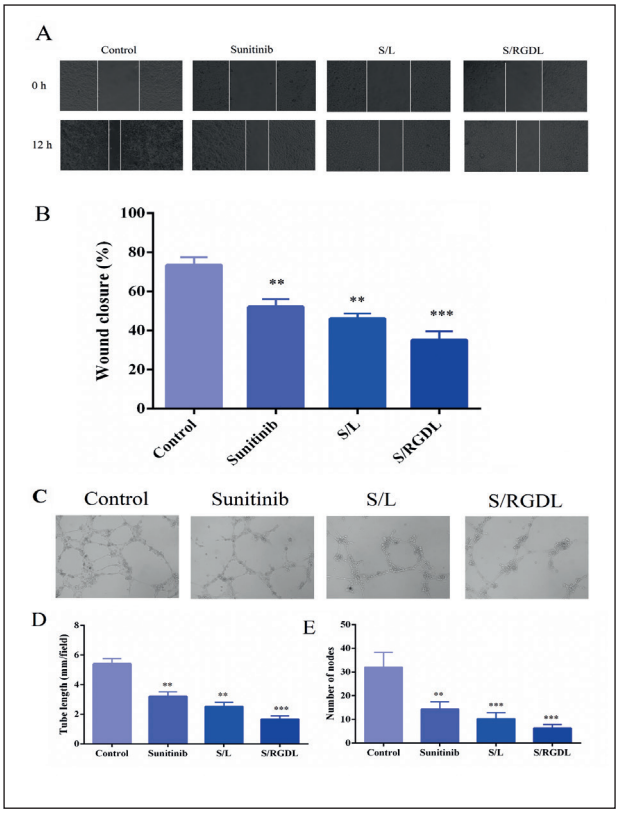

Figure 4: S/RGDL prevents the migration of UM-UC-14 cells and inhibits the angiogenesis of endothelial cells in vitro. (A). Wound closure assays were performed, and the representative wound healing images of UM-UC-14 cells treated with sunitinib, S/L, or S/RGDL at the indicated times were shown. (B). Quantification of the extent of wound closure. (C) HUVECs treated with the indicated drugs were plated onto Matrigel to induce tube formation, and photographs were taken 3 h later. Representative images were exhibited, and tube length (D) and node number (E) were analyzed. Results are presented as mean ± SD, **indicates $p<0.01$, and ***indicates $p<0.001$.

Acute toxicity evaluation and inhibition of angiogenesis

To make sure in-vitro biocompatibility, it is important to perform in-vivo acute toxicity tests in animals. After 14 days of observation, no serious adverse effects or signs of morbidity were found in any animal in all groups. The above results showed that S/RGDL could inhibit UM-UC-14 cell proliferation, migration and suppressed endothelial cell angiogenesis in vitro.

To explore the targeting ability and inhibition of angiogenesis of S/RGDL in renal carcinoma in vivo, antitumor effect was evaluated in UM-UC-14-beared mice. As shown in Figure 5A, S/L could inhibit the proliferation of renal carcinoma more than the sunitinib group due to the nonspecific targeting of liposomes. While the targeted liposome S/RGDL gave a better inhibition than the other two groups (Figure 5B).

To further confirm whether treatment of sunitinib formulations impaired the angiogenesis capacity in tumors isolated from mice, Immunoblot assays were performed. The data confirmed the effective downregulation of CD31, an endothelial cell marker, in tumor tissues from the three groups (Figure 5C).

Similarly, we also noticed that the expression of VEGF, which was critical in the angiogenesis process, was obviously decreased upon the treatment of S/RGDL, further suggested the impaired angiogenesis capacity.

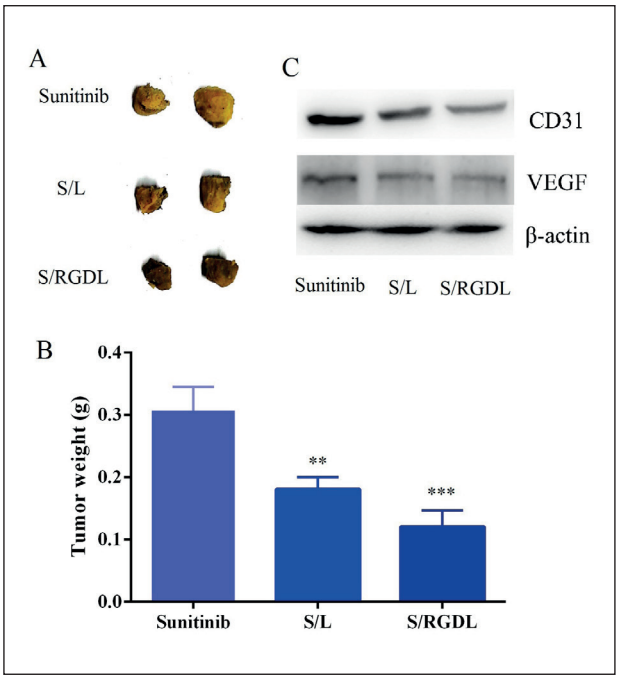

Figure 5: In vivo inhibition of angiogenesis (A) Representative tumor images were shown, (B) Tumor weight was compared between the three groups, (C) Immunoblot assays showed the expression level of the indicated proteins tumor tissues isolated from mice. Results are presented as mean ± SD, **indicates $p<0.01$, and ***indicates $p<0.001$.

Discussion

Renal carcinoma is a very high degree of malignancy with a very high incidence and mortality.1 Angiogenesis is an important part of tumor progression, and the important effect on angiogenesis is reflected in the regulation of cell proliferation and migration[10]. Sunitinib is a multi-target angiogenesis inhibitor through the inhibition of multiple tyrosine kinases such as VEGFR1 and PDGFR(11). However, the obvious limitation of sunitinib has also been noticed.

In this study, a RGD-modified derivative 11 was designed and prepared, which was used as a ligand in the liposomal drug delivery system. The sunitinib-loaded liposome S/RGDL was characterized for particle size, zeta potential, encapsulation efficiency, release profile, stability, and hemolysis in vitro, and the results indicated the liposome had superior properties. It was found that S/RGDL could significantly inhibit the formation of tubular structures and further found that it had important effects on the proliferation and migration of tumor cells. Interestingly, we also found the S/RGDL could obviously promote the anti-tumor and anti-angiogenesis effects for the treatment of renal carcinoma, confirmed by a series of in vitro and in vivo assays, which might be caused by the multi-anti-angiogenesis effect upon sunitinib and RGD peptide combination treatment. In fact, this work provided the potential that S/RGDL could serve as a possible manner to improve the clinical therapeutic effects of renal carcinoma through promoting anti-tumor and anti-angiogenesis capacity.

In this study, we have developed a RGD-modified liposomal drug delivery system. The liposome was capable of recognizing the receptor of integrin $\alpha v\beta 3$ via RGD peptide on the surface of the particles. S/RGDL possesses good stability in vitro. It was noticed that S/RGDL obviously suppressed the proliferation capacity both in vitro and in vivo compared to S/L or sunitinib, which might be due to the dual-antiangiogenesis of both sunitinib and RGD peptide. Generally, this work presented a way that S/RGDL may be used as potential means to improve the therapeutic efficiency of renal carcinoma via enhancing target and anti-tumor ability.

References

1) Gold S, Taylor J, Margulis V. Renal cell carcinoma with inferior vena cava thrombus: did we make progress in oncologic outcomes and complications? Current Opinion in Urology 2023; 33: 142-146.
2) Bersanelli M, Rebuzzi SE, Roviello G, Catalano M, Brunelli M, Rizzo M. Immune checkpoint inhibitors in non-conventional histologies of renal-cell carcinoma. Human Vaccines & Immunotherapeutics 2023; DOI: 10.1080/21645515.2023.2171672.
3) Hirashita T, Iwashita Y, Endo Y, Fujinaga A, Shin T, Mimata H, Inomata M. How Should We Treat Pancreatic Metastases from Renal Cell Carcinoma? A Meta-Analysis. World Journal of Surgery 2021; 45: 2191-2199.
4) Lugano R, Ramachandran M, and Dimberg A (2019). Tumor angiogenesis: causes, consequences, challenges and opportunities. Cell Molecular Life Science 2020; 77: 1745-1770.
5) Unterleuthner D, Neuhold P, Schwarz K, Janker L, Neuditschko B, Nivarthi H, Crncec I, Kramer N, Unger C, Hengstschlager M, Eferl R, Moriggl R, Sommergruber W, Gerner C, and Dolznig H. Cancer-associated fibroblast-derived WNT2 increases tumor angiogenesis in colon cancer. Angiogenesis 2019; 23: 159-177.
6) Chen CY, Lin YJ, Wang CCN, Lan YH, Lan SJ, and Sheu MJ. Epigallocatechin-3-gallate inhibits tumor angiogenesis: involvement of endoglin/Smad1 signaling in human umbilical vein endothelium cells. Biomed Pharmacother 2019; 120: 109491.
7) Kim DH, Park S, Kim H, Choi YJ, Kim SY, Sung KJ, Sung YH, Choi CM, Yun M, Yi YS, Lee CW, Kim SY, Lee JC, and Rho JK. Tumor-derived exosomal miR-619-5p promotes tumor angiogenesis and metastasis through the inhibition of RCAN1.4. Cancer Letters 2020; 475: 2-13.
8) Guillaume Z, Auvray M, Vano Y, Oudard S, Helley D, Mauge L. Renal Carcinoma and Angiogenesis: Therapeutic Target and Biomarkers of Response in Current Therapies. Cancers 2022; 14: 6167.
9) Zhu Y, Liu X, Wang Y, Pan Y, Han X, Peng B, Zhang X, Niu S, Wang H, Ye Q, Gu Y, Gao S. DMDRMR promotes angiogenesis via antagonizing DAB2IP in clear cell renal cell carcinoma. Cell Death & Disease 2022; 13: 456.
10) Haaker L, Tryssesoone L, Renders I, Verbiest A, Lerut E, Baldewijns M, Bourgain C, Roussel E, Van den Bulck H, Wynendaele W, Laguerre B, Rioux-Leclercq N, Oudard S, Laenen A, Debruyne PR, Albersen M, Beuselinck B. Bone metastasis is associated with poor prognosis in metastatic papillary renal cell carcinoma patients treated with first agent angiogenesis inhibitors. Urologic Oncology 2020; 38: 686.e1.
11) Yu Y, DuBois SG, Wetmore C, and Khosravan R. Physiologically Based Pharmacokinetic Modeling and Simulation of Sunitinib in Pediatrics. AAPS Journal 2020; 22: 31.
12) Su H, Xue Z, Feng Y, Xie Y, Deng B, Yao Y, Tian X, An Q, Yang L, Yao Q, Xue J, Chen G, Hao C, and Zhou T. N-aryl piperazine-containing compound (C2): An enhancer of sunitinib in the treatment of pancreatic

cancer, involving D1DR activation. Toxicology and Applied Pharmacology 2019; 384: 114789.
13) Shi H, Sun Y, He M, Yang X, Hamada M, Fukunaga T, Zhang X, and Chang C. Targeting the TR4 nuclear receptor-mediated lncTASR/AXL signaling with tretinoin increases the sunitinib sensitivity to better suppress the RCC progression. Oncogene 2020; 39: 530-545.
14) Uhl C, Markel M, Broggini T, Nieminen M, Kremenetskaia I, Vajkoczy P, and Czabanka M. EphB4 mediates resistance to antiangiogenic therapy in experimental glioma. Angiogenesis 2018; 21: 873-881.
15) Terao S, Acharya B, Suzuki T, Aoi T, Naoe M, Hamada K, Mizuguchi H, Gotoh A. Improved gene transfer into renal carcinoma cells using adenovirus vector containing RGD motif. Anticancer Research 2009; 29: 2997-3001.
16) Sorolla A, Wang E, Clemons TD, Evans CW, Plani-Lam JH, Golden E, Dessauvagie B, Redfern AD, Swaminathan-Iyer K, and Blancafort P. Triple-hit therapeutic approach for triple-negative breast cancers using docetaxel nanoparticles, EN1-iPeps and RGD peptides. Nanomedicine 2019; 20: 102003.
17) Friedlander M, Brooks PC, Shaffer RW, Kincaid CM, Varner JA, and Cheresh DA. Definition of two angiogenic pathways by distinct alpha v integrins. Science 1995; 270: 1500-1502.
18) Brooks PC, Clark RA, and Cheresh DA. Requirement of vascular integrin alpha v beta 3 for angiogenesis. Science 1994; 264: 569-571.
19) Matej J, Neva PL, Peri M and Alenka SV. Fluid optimization in pancreas surgery. Signa Vitae 2019; 15: 45-51.
20) Yockman JW, Kim WJ, Chang CW, Kim SW. Non-viral delivery of interleukin-2 and soluble Flk-1 inhibits metastatic and primary tumor growth in renal cell carcinoma. Gene Therapy 2007; 14: 1399-1405.
21) Beekman KW, Colevas AD, Cooney K, Dipaola R, Dunn RL, Gross M, Keller ET, Pienta KJ, Ryan CJ, Smith D, and Hussain M. Phase II evaluations of cilengitide in asymptomatic patients with androgen-independent prostate cancer: scientific rationale and study design. Clinical Genitourinary Cancer 2006; 4: 299-302.
22) Zhao Y, Peng Y, Yang Z, Lu J, Li R, Shi Y, Du Y, Zhao Z, Hai L, and Wu Y. pH-redox responsive cascade-targeted liposomes to intelligently deliver doxorubicin prodrugs and lonidamine for glioma. European Journal of Medicinal Chemistry 2020; 235: 114281.
23) Zhao Z, Chen C, Xie C, and Zhao Y. Design, synthesis and evaluation of liposomes modified with dendritic aspartic acid for bone-specific targeting. Chemistry and Physics of Lipids 2020; 226: 104832.
24) He XJ, Qian YN, Wu CL, Feng JY, Sun XS, Zheng QX, Li XK, and Shen JL. Entropy-Mediated High-Entropy MXenes Nanotherapeutics: NIR-II-Enhanced Intrinsic Oxidase Mimic Activity to Combat Methicillin-Resistant Staphylococcus Aureus Infection. Advanced Materials 2023, DOI: 10.1002/adma.202211432.
25) He XJ, Hou JT, Sun XS, Jangili P, An JS, Qian YN, Kim JS, and Shen JL. NIR-II Photo-Amplified Sonodynamic Therapy Using Sodium Molybdenum Bronze Nanoplatform against Subcutaneous Staphylococcus Aureus Infection. Advanced Functional Materials 2022; 32: 2203964.
26) He XJ, Koo S, Obeng E, Sharma A, Shen JL, and Kim JS. Emerging 2D MXenes for antibacterial applications: Current status, challenges, and prospects. Coordination Chemistry Reviews 2023; 492: 215275.
27) Li C, Zhang Y, Chen G, Hu F, Zhao K, and Wang Q. Engineered Multifunctional Nanomedicine for Simultaneous Stereotactic Chemotherapy and Inhibited Osteolysis in an Orthotopic Model of Bone Metastasis. Advanced Materials 2017; 29: 1605754.

.

Corresponding Authors:
Huibing Li
Email: researcherlhb@163.com
(China)
Changyi Quan
Email: quanchangyi@tmu.edu.cn
(China)